Original Article

Journal of Drought and Climate change Research (JDCR)

Summer 2024, Vol. 2, No. 6, pp 93-104

10.22077/jdcr.2024.7376.1061

Measuring Discharge in a Shallow River in an Arid Area solely using an Unmanned Aerial Vehicle

Farhad Akbarpour[1*], Mohammad Adel Khorasani Nejad[2], Shervin Shahriari[3], Mostafa Rahmanshahi[4]

1. River Conservation Engineer, Tehran Regional Water Company, Tehran, Iran.
2. PhD candidate, Islamic Azad University, Science and Research Branch, Tehran, Iran.
3. PhD graduate, Institute of Hydraulic Engineering and Water Resources Management, Graz University of Technology, Austria.
4. Postdoctoral fellow, Hong Kong Polytechnic University, Hong Kong.

*** corresponding author: farhad.akbarpoor@gmail.com**

Keywords:
Discharge, LSPIV, UAVs, Bathymetry, Large Eddy PIV.

Received:
02 March 2024

Revised:
28 April 2024

Accepted:
11 May 2024

Abstract

Unmanned Aerial Vehicles (UAVs) have recently been applied for river flow measurement. In this research, UAV images were first used to acquire surface velocity fields of a small river in an arid area in Iran based on the principles of Large Scale Particle Image Velocimetry (LSPIV). Subsequently, Large Eddy PIV method was applied on the instantaneous velocity data to obtain turbulent kinetic energy dissipation rates along a selected cross section of the experimented river. In addition, a UAV image was captured and processed to gain the bed material grain size distribution and consequently the Manning roughness coefficient. The resulted gradation curve matched the graph given by sieve analysis with an accuracy of nearly 7.8 percent. Moreover, an equation combining the acquired surface velocity, dissipation rates and Manning coefficient was used to estimate the river bathymetry. Although, the evaluated bathymetry does not fit the surveyed cross section very well, the average predicted depth matches the measured mean depth with a high precision. Finally, the river flow rate calculated using the information solely resulted from UAV images fitted the measured discharge with an accuracy of 5 percent proving the described framework to be a very effective method for primary river flow evaluation especially when supplementary depth measurement is not feasible.

How to cite this article:
Akbarpour, F., Khorasani Nejad, M.A., Shahriari, Sh., & Rahmanshahi, M. (2024). Measuring Discharge in a Shallow River in an Arid Area solely using an Unmanned Aerial Vehicle. *Journal of Drought and Climate change Research* (JDCR), 2(6), 93-104. 10.22077/jdcr.2024.7376.1061

Introduction

Flow discharge is a very important feature of rivers in arid areas for water resources management and allocation and also for designing flood control schemes in the case of extreme hydrological events. Especially, under drought conditions it is crucial to measure water flowing in rivers as accurate as possible. Most stream gages currently being operated in Iran are based on stage-discharge method which is of course of major deficiencies. The rating curves are mainly drawn based on measurements conducted under low flow conditions and extrapolated for higher amounts of discharge. Thus, discharge records for flood events are normally subject to significant errors. Therefore, in the situation of water scarcity where annual average precipitation in Tehran Province hardly reaches 300 millimeters, seeking alternative approaches with higher accuracies deems essential for sustainable management of available water resources. Meanwhile, image-based velocity measurement methods also referred to as near field remote sensing techniques have recently been widely utilized by water professionals.

Large Scale Particle Image Velocimetry (LSPIV) is among the most frequently used imagery methods applied under different conditions from very low flow to flood events. The method firstly suggested and experimented by Fujita et al, 1998 in Japan is built essentially upon particle pattern recognition formed on flow surface in consecutive images under natural light exposures. The principles of LSPIV are similar to the conventional PIV excluding the necessity of laser application for flow visualization while larger flow fields even up to hundreds of meters might be measured.

In addition to flow measurement, LSPIV has also been used to investigate time-averaged surface flow patterns (Bieri et al., 2009 Kantoush et al., 2011; Sutarto, 2015), turbulence features on the free surface (Orlins and Gulliver, 2000; Albayrak and Lemmin, 2007; Fox and Patrick, 2008) and the effect of free surface turbulence on the air- water gas transfer (Mc Kenna and Mc Gillis, 2004).

For flow discharge measurement in waterways using image-based techniques, two supplementary data sets are necessary to acquire. Firstly, the mean velocity at the surface obtained through processing the recorded images ought to be converted to depth-averaged velocity. This is usually achieved by multiplying the surface velocity by a constant coefficient (the velocity index or coefficient) which is well established to be equal to 0.85. However, it is to be borne in mind that the value of 0.85 is proposed for deep hydraulically smooth channels where it is possible to assume a logarithmic velocity profile (Welber et al., 2016). In some studies, LSPIV has been used to measure surface velocity to investigate the velocity index (Polatel, 2006; Welber et al., 2016; Novak et al., 2017). Several researchers have found different values for this index. For instance, Weitbrecht et al (2002) obtained 0.805 for a smooth bed. Lee & Julien (2006) obtained values 0.61 and 0.79 for a gravel bed river and clay bed canal, respectively. Novak et al (2017) found values between 0.73 and 0.89 for a horizontal glass bed flume and values 0.72 to 0.85 for a concrete flume with a slope of 0.001 where in both cases VI increases with depth. Huang et al (2018) found 0.737 for the gravel bed Yufeng Creek. Akbarpour et al (2020) obtained values 0.61 to 0.78 for steep slopes (2, 6 and 10 percent) of a flume roughened with identical glass spheres ideally representing gravel bed rivers.

The variations in the velocity index might be attributed to the parameters such as bed roughness, relative submergence or aspect ratio and flow regime (Polatel, 2006). Akbarpour et al (2020) also showed that the index is increased as the bed gradient increases and proposed an equation relating the index to the relative roughness and the slope. Johnson and Cowen (2017) in a different approach expressed the possibility of evaluating the velocity index by estimating the shear velocity from the turbulence spatial spectra and the recorded surface velocity and consequently predicting the velocity power-law exponent. Gunawan et al (2012) proved that the coefficient also varies in the transverse direction along the cross section due to the variations in the cross sectional shape of the reach, local vegetation and stage.

In addition to the velocity index, channel bathymetry or depth should also be known when measuring river flow rate using LSPIV. Johnson and Cowen (2016) suggested that through measuring surface turbulence metrics and more specifically integral length scales it is feasible to estimate the flow depth. Jin and Liao (2019) applied LSPIV to evaluate statistics of surface turbulence of a natural river and correlated the flow depth with the turbulent kinetic energy dissipation rate of the flow surface. They suggested that the water depth along the cross section might be estimated using the river Manning's n and the dissipation rate obtained from processing the sequence of surface images. On the other hand, image processing techniques have been utilized throughout the recent years to determine grain size distribution of river bed material (Butler et al., 2001: Graham et al., 2005; Buscombe et al., 2010; Spada et al., 2018). Moreover, some researchers have applied Unmanned Aerial Vehicles as platforms for cameras to be mounted on for the same purpose (Vázquez-Tarrío et al., 2017; Lang et al., 2020).

Recently efforts have been made to explore the applicability of airborne velocimetry methods to measure stream flow discharge without any supplementary bathymetry measurements. Detert et al (2017) introducing applications of airborne image velocimetry (AIV) used an off-the-shelf action camera mounted to a lowcost quadcopter to determine a small rivers' surface velocity field, bathymetry, and its flow discharge. They applied particle image velocimetry to compute flow velocities. In order to remotely determine the river bathymetry they used structure from motion (SfM) and MultiView Stereo (MVS) techniques applied to the UAV images. Kinzel and Legleiter (2019) measured the surface velocity field and bathymetry of a river employing two small Unmanned Aerial Systems (sUAS) equipped with a thermal infrared camera and a polarizing lidar, respectively. Eltner et al (2020) introduced a remote sensing workflow for automatic flow velocity calculation and discharge estimation using the depth-averaged velocity obtained from application of PTV and the wetted cross section derived from SfM and multi-media photogrammetry applied to UAV imagery. In this paper a UAV was employed to measure surface velocity of a shallow river flowing in an arid region located in the south of Tehran the capital city of Iran. The results show that through the analysis of the acquired images based on Large Scale Particle Image Velocimetry principles an accurate surface velocity field was obtained. In addition, the airborne device was used to acquire few images from the dry river bank adjacent to the wetted section. Image processing techniques

were later used to determine the bed grain size distribution and subsequently the Manning's n. Moreover, Large Eddy PIV method was used to calculate turbulence dissipation rate on flow surface. Finally, a simple method was proposed to estimate the river bathymetry enabling the calculation of river discharge. The results show that the employed framework yields acceptable values for the river flow rate under the experimented conditions.

Material and Methods

1. Study Area

This study was conducted in a rather straight short reach of the river Kan located in the south of Tehran Province, Iran at 51° 19' 04" E and 35° 32' 58" N (Figure 1). The field measurement was carried out on May 28, 2020 when the river flow rate according to the current meter measurement was equal to 2.82 m^3/s. The site consists of a transect (shown with red dashed line in Figure 1) where the bathymetry of the river channel was manually surveyed by a wading meter at a 0.5-m interval. The channel top width at the time of survey was 9.1 m at the selected transect. Bed materials are primarily composed of gravel without the presence of large boulders.

2. LSPIV measurements

The measurement device was a DJI Phantom 4 Pro which has a camera capable of shooting 4k video at 60 fps and capturing 20 megapixel stills on board. In our experiment the camera recorded videos in a resolution of 1920×1080 at 30 fps. The drone is equipped with a stabilizing gimbal to diminish camera movements to an acceptable level for image processing. The camera was held at a nadir position as much as possible throughout the image capturing period.

Fig 1. Location and an aerial image of the study area. The blue circles and the red dashed line on the right hand image show location of the GCPs and the surveyed cross section.

The airborne image data were captured at a flying height of about 20 meters. Video sequences were converted into individual frames prior to the image processing. Since the camera was kept quite stable during the measurement campaign image co-registration to remove the camera movements was not necessary.

Four ground control points (GCPs) were distributed uniformly on both riversides whose coordinates were required during the image processing. The geocoordinates were recorded by a Garmin eTrex which was used three times for each GCP to improve its accuracy. However, final accuracy of the GCPs' positions is estimated to be ±2-3 m which is quite poor but sufficient for the current purpose.

It is also advised to use tracer particles in LSPIV for the image processing step. The tracers need to be somewhat lighter than water to be floating on the flow surface while not too light to represent the flow behavior passively. In this study pieces of walnut wood with a specific density of 0.7 and an average size of 3×3 cm and thickness of about 1 cm were manually distributed on the water surface to act as the flow tracers. However there are evidences that natural tracing might also work under some circumstances. For unseeded applications, natural tracers such as foams, bubbles or superficial reflection patterns due to surface deformations might be used for PIV processing (Jin and Liao, 2019; Bentazzo et al., 2017). In this research, the MATLAB toolbox PIVlab was used to process the images (Thielicke and Stamius, 2014). PIVlab and most PIV software packages are based on cross correlation algorithm where the images are first divided into a number of interrogation areas (IA). Since this algorithm is in fact based on the recognition of the patterns formed by the tracer particles in each IA, for each of the two consecutive images, the correlation coefficient of each IA in the first image with the adjacent IAs in a certain area in the second image is calculated for pattern recognition. Then the IA with the largest value of the correlation coefficient is determined as the destination of the tracer particles displacement. Having the direction and value of the displacement within the time *dt*, the velocity vector is obtained for the desired IA. This process continues until the velocity vector calculation for all IAs in the image is performed and thus the velocity field for each two consecutive images is achieved. In this study, the video recording was performed for a duration of 60 seconds at the rate of 30 fps and in total 1800 images were acquired. Before starting the main stage of image processing the region of interest (ROI) was cropped from the original images by masking the unwanted parts on either sides of the river. Then the raw images were converted to grayscale, contrast-limited adaptive histogram equalization (CLAHE) was used to enhance the images contrast, and a high-pass filtering was applied. According to the physical dimensions of the measurement plane the size of each pixel would be equal to 16.5 mm. In the next step, the images were calibrated using the GCPs' recorded coordinates and then the image evaluation settings were introduced. In this study, multi-pass cross correlation method via Fast Fourier Transform (FFT) was used where initially the image evaluation starts with a large IA (128 × 128 pixels) and the results are used for smaller IAs (eventually 16 × 16 pixels) and velocity vectors are obtained for each IA. Finally, in post processing bad vectors are omitted by defining the minimum and maximum acceptable velocity values and the velocity fields are calculated.

3. Flow depth estimation from surface velocity fluctuations and Manning coefficient

Jin and Liao (2019) assumed that Law-of-Wall equation for the vertical profile of the dissipation rate can be extended to the free surface, combined it with Manning-Strickler equation and proposed the

following equation for water depth estimation in rivers involving the turbulent surface velocity measurement and the Manning's roughness coefficient, n :

$$H = \frac{K^2 U_s^2 n^2 g}{(k\varepsilon_s)^{2/3}} \quad (1)$$

Where for the estimation of depth (H), having the surface velocity (U_s) and surface dissipation rate (ε_s) is necessary and g is gravitational accretion and k is von Karman constant equal to 0.41. The velocity index (K) was taken equal to the conventional 0.85 value since we do not have any preceding knowledge of the water depth to benefit from the existing relationships.

3.1. Remote estimation of the Manning's n

In order to evaluate the Manning's n we captured a supplementary image from the left bank side of the studied river using the aforementioned drone from a point 5 meters above the surface. A square wooden frame (40 by 40 cm) was placed over the selected area to ensure the possibility of scale definition. FHWA Hydraulic Toolbox was used to extract bed gradation information from the digital image. The workflow utilized by the program and the captured digital image are shown in Figure 2. As it could be seen in the figure, Grain size distribution will be the outcome of the program. Having the bed material gradation information and using one of the existing empirical equations the Manning coefficient could be estimated from the bed grain size already estimated. In this paper, since we would intend to propose a method to evaluate the flow rate without direct depth measurement and considering the fact that the experimented reach is quite straight without any vegetation roughness, Strickler (1923) formula was used to convert grain size to roughness coefficient as follows:

$$n = 0.015\, D_{50}^{1/6} \quad (2)$$

1.1.

3.2. Surface turbulence dissipation rate approximation using Large Eddy PIV method

Sheng et al (2000) proposed Large Eddy PIV inspired by the concept of Large Eddy Simulation (LES). Since in PIV measurements image correlation is applied on finite grid sizes, it is similar to LES filtering where the instantaneous velocity is decomposed into a resolved velocity $\overline{U_i}$, and an unresolved velocity U_i:

$$u_i = \bar{U}_\iota + \breve{u}_\iota \quad (3)$$

The turbulence dissipation rate can be estimated as follows:

$$\varepsilon \approx -2\langle \tau_{ij} \bar{S}_{ij} \rangle \quad (4)$$

Where $\langle\rangle$ denotes ensemble averaging and $\bar{S}_{ij}$ is the strain rate tensor defined as:

$$\bar{S}_{ij} = \frac{1}{2}\left(\frac{\partial \bar{U}_j}{\partial x_i} + \frac{\partial \bar{U}_i}{\partial x_j}\right) \quad (5)$$

And τ_{ij} is the stress tensor often obtained using Smagorinski model: $\tau_{ij} = -C_s^2 \Delta^2 |\bar{S}| \bar{S}_{ij}$ where is the interrogation area size in PIV and C_s is Smagorinski constant equal to 0.17. In this paper this method is used to approximate surface turbulence dissipation rate ε_s.

Results and Discussion

1. Surface velocity field

The two dimensional time-averaged surface velocity field of the experimented river reach is depicted in Figure 3.

As it could be observed the mean surface velocity is higher tending to the left hand side of the channel which is quite sensible because the corresponding depth at that part is larger in comparison to other regions. The velocity gradient on the left

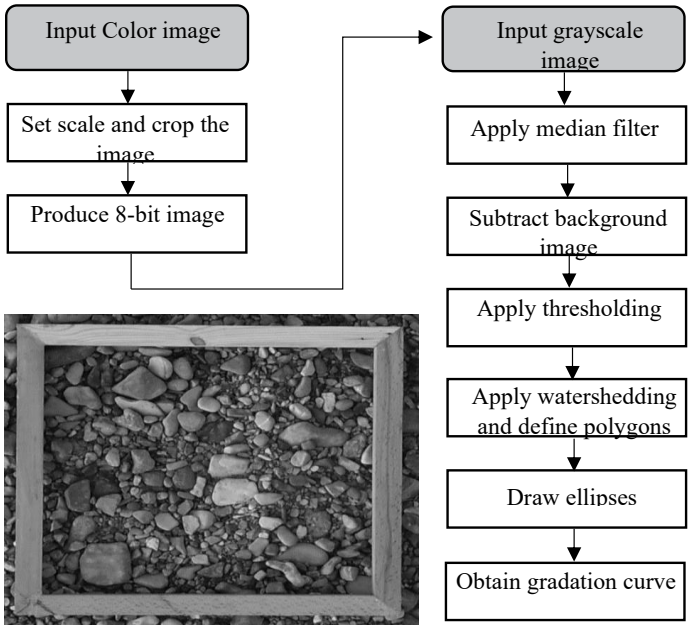

Fig 2- The underlying workflow used to estimate bed gradation from the digital image (a), the image captured at 5-meter height on the left bank of the river reach (b).

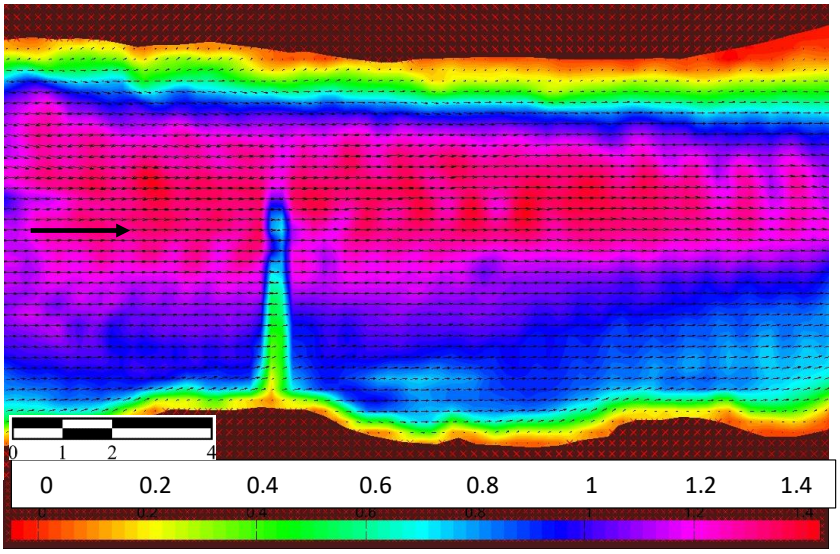

Fig 3- 2D surface velocity field of the experimented river reach.

bank is more gradual because of its gentle slope while on the right bank we observe a sharper gradient due to the abrupt slope of the river edge. The position of the wading meter is also detected in the image processing as a narrow bar with a much smaller velocity appearing on the velocity field.

The lateral variation of the surface velocity against the depth-averaged velocity measured by the current meter is depicted in Figure 4. It is obvious that on the right hand side of the cross section the surface and depth-averaged velocities agree very

well. However, in the left hand side the depth-averaged velocity has an abrupt increase at y= 0.2 which is not detected accordingly by LSPIV. The reason might be inappropriate distribution of seeding particles or unwanted light reflections at that area.

2. **Manning roughness coefficient**

As explained in section (2-3-1) image processing was applied to approximate river bed gradation. In order to be able to compare the results, a sample sediment patch was taken from the same place as the imaged area. Figure 5 shows the gradation graphs obtained from sieve analysis and image processing. The results agree very well with the measured gradation data with a RMSE equal to 7.8 %. The calculated median grain size (D_{50}) obtained through the image analysis equals 24.9 mm and according to equation (2) the Manning roughness coefficient is estimated to be 0.025.

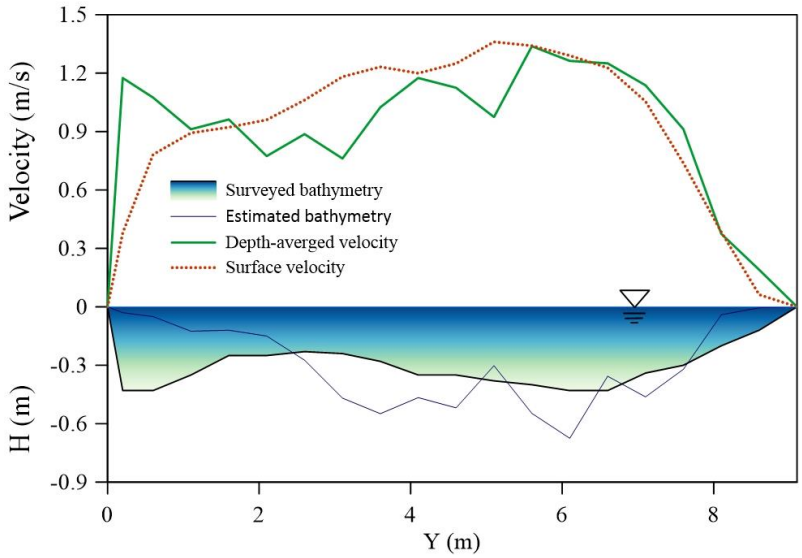

Fig 4. Surface velocity (LSPIV) versus depth-averaged velocity (current meter) and also comparison of the estimated bathymetry using equation 1 against the surveyed cross section.

3. River bathymetry and discharge

Following equation (1) and taking Manning's n equal to 0.025 as obtained from image processing techniques and inserting the surface turbulence dissipation rates calculated from Large Eddy PIV method, the values of flow depth across the selected cross section were calculated as shown in Figure 4. Except from the near end of the section the general trend of the estimated depth variation agrees to some extent with the measured bathymetry. However, the estimated bathymetry shows more fluctuations and with the exception of the first two meters mostly higher depth values. The average depth of the section resulted from equation (1) is 0.27 m while the average depth according to the surveyed data is 0.288 m showing an error of nearly 6 percent. Thus, the applied method in this paper proves to be quite adequate to roughly estimate the mean water depth. Whilst, to be able to depend on the bathymetry obtained from the method more investigations ought to be carried out.

Moreover, the river discharge was calculated using the velocity-area method as follows with the measured surface velocity gained from LSPIV multiplied by

K=0.85 and the water depth distribution estimated by equation (6):

$$Q = \int_0^w KU_s(y)H(y)dy \quad (6)$$

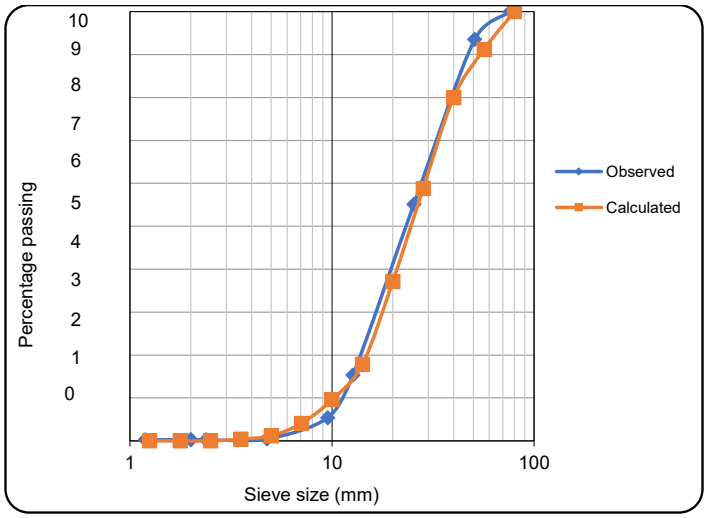

Fig 5. Evaluated (image processing) versus measured (sieve analysis) bed sediment gradation curves.

The calculated flow rate based on equation (6) equals 2.67 m^3/s which is approximately 5 percent lower than the measured discharge of 2.82 m^3/s using the current meter. Therefore, the proposed method which only relies on the data acquired from a UAV including surface velocity and subsequently surface turbulence dissipation rate distributions and also bed material gradation obtained through image processing techniques shows a great potential to be applied for primary river discharge estimations especially once it is not feasible to wade the river bathymetry.

Conclusions

A UAV was used in this paper to estimate both mean velocity and water depth distribution (bathymetry) in a small shallow river in an arid area in Iran solely by imaging the free surface. According to the surface velocity distribution obtained from the application of LSPIV method, the surface velocity in the left half (with reference to the flow direction) of the observed river reach is quite higher than that of the right half. The trend recorded by the current meter also shows that the depth-averaged velocities are larger in the left half confirming the results of the surface velocity measurement. With the exception of the first one meter and the last two meters of the cross section, for the majority of the section width the depth-averaged velocity is lower than the surface velocity which is consistent with the previous findings indicating dip phenomenon.

Bed grain size distribution was also approximated using image processing techniques. The estimated gradation graph shows a very good agreement with the measured curve with a RMSE of 7.8 percent. Subsequently, the Manning roughness coefficient was calculated from the calculated median grain size (D_{50}) using Strickler formula showing a value equal to 0.025 which is around 16 percent lower than the calculated 0.029 from the measured data based on Manning equation. Hence, using the gradation acquired from drone imagery in a gravel bed river without major large roughness elements and

vegetation yielded an acceptable Manning coefficient.

The application of equation (1) proposed by Jin & Liao to estimate lateral water depth distribution using the Manning coefficient obtained through image processing and surface turbulence dissipation rate distribution calculated from Large Eddy PIV did not result in an identical bathymetry with the surveyed cross section. However, the resulted average depth is really close to the mean surveyed depth with a 6 percent error.

The discharge calculated from the introduced methodology agreed very well with the measured value with a distinction of approximately 5 percent. Therefore, it is possible to take advantage of the proposed methodology to estimate velocity, depth and consequently discharge using solely a UAV with an acceptable precision without any supplementary measurement for bathymetry under similar conditions to the experimented river reach.

Finally, in order to enhance the proposed framework, more laboratory and field experiments should be conducted in the future to explore correlations between flow depth and turbulence metrics including integral length scales and surface dissipation rate of turbulent kinetic energy.

Acknowledgements

The authors would like to thank the kind support of Roodkhiz Water and Environment Company for providing the UAV and their participation in river flow measurement.

References

Akbarpour, F., Fathi-Moghadam, M., & Schneider, J. (2020). Application of LSPIV to measure supercritical flow in steep channels with low relative submergence. *Flow Measurement and Instrumentation*, *72*, 101718. https://doi.org/10.1016/j.flowmeasinst.2020.101718.

Albayrak, I., & Lemmin, U. (2007). Large scale PIV-measurements on the water surface of turbulent open channel flow. *18ème Congrès Français de Mécanique*, August 27-31., Grenoble, France. https://hal.science/hal-03358595.

Benetazzo, A., Gamba, M., & Barbariol, F. (2017). Unseeded large scale PIV measurements corrected for the capillary-gravity wave dynamics. *Rendiconti Lincei*, *28*(2), 393-404. https://doi.org/10.1007/s12210-017-0606-2

Bieri, M., Jenzer, J., Kantoush, S.A., & Boillat, J. L. (2009). Large scale particle image velocimetry applications for complex free surface flows in river and dam engineering. *33rd IAHR Congress Proc*. British Columbia, Vancouver, 604-611.

Buscombe, D., Rubin, D.M., & Warrick, J.A. (2010). A universal approximation of grain size from images of noncohesive sediment. *Journal of Geophysical Research: Earth Surface, 115*(F2). https://doi.org/10.1029/2009JF001477.

Butler, J.B., Lane, S.N., & Chandler, J.H. (2001). Automated extraction of grain-size data from gravel surfaces using digital image processing. *Journal of hydraulic research*, *39*(5), 519-529. https://doi.org/10.1080/00221686.2001.9628276

Detert, M., Johnson, E.D., & Weitbrecht, V. (2017). Proof-of-concept for low-cost and non-contact synoptic airborne river flow measurements. *International Journal of Remote Sensing*, *38*(8-10), 2780-2807. https://doi.org/10.1080/01431161.2017.1294782

Eltner, A., Sardemann, H., & Grundmann, J. (2020). Flow velocity and discharge measurement in rivers using terrestrial and un-

manned-aerial-vehicle imagery. *Hydrology and Earth System Sciences*, *24*(3), 1429-1445. https://doi.org/10.5194/hess-24-1429-2020

Fox, J.F & Patrick, A. (2008). Large-scale eddies measured with large scale particle image velocimetry. *Flow Measurement and Instrumentation* (19), 283–291. https://doi.org/ 10.1016/j.flowmeasinst.2008.01.003.

Fujita, I., Muste, M., & Kruger, A. (1998). Large-scale particle image velocimetry for flow analysis in hydraulic engineering applications, *Journal of Hydraulic Research*, 36(3), 397-414. https://doi.org/10.1080/00221689809498626.

Graham, D.J., Rice, S.P., & Reid, I. (2005). A transferable method for the automated grain sizing of river gravels. *Water Resources Research*, *41*(7). https://doi.org/10.1029/2004WR003868.

Gunawan, B., Sun, X., Sterling, M., Shiono, K., Tsubaki, R., Rameshwaran, P., Knight, D.W., Chandler, J.H., Tang, X., & Fujita, I. (2012). The application of LSPIV to a small irregular river for inbank and overbank flows. *Flow Measurement and Instrumentation*, *24*, 1-12. https://doi.org/10.1016/j.flowmeasinst.2012.02.001.

Huang, W.C., Young, C.C., & Liu, W.C. (2018). Application of an automated discharge imaging system and LSPIV during typhoon events in Taiwan. *Water*, *10*(3), 280. DOI:10.20944/preprints201802.0089.v1

Jin, T., & Liao, Q. (2019). Application of large scale PIV in river surface turbulence measurements and water depth estimation. *Flow Measurement and Instrumentation*, *67*, 142-152. https://doi.org/10.1016/j.flowmeasinst.2019.03.001.

Johnson, E.D., & Cowen, E.A. (2016). Remote monitoring of volumetric discharge employing bathymetry determined from surface turbulence metrics. *Water Resources Research*, *52*(3), 2178-2193. https://doi.org/10.1002/2015WR017736

Johnson, E.D., & Cowen, E.A. (2017). Remote determination of the velocity index and mean stream wise velocity profiles. *Water Resources Research*, *53*(9), 7521-7535. https://doi.org/10.1002/2017WR020504

Kantoush, S.A., Schleiss, A.J., Sumi, T., & Murasaki, M. (2011). LSPIV implementation for environmental flow in various laboratory and field cases. *Journal of Hydro-environment Research*, (5), 263-276. https://doi.org/10.1016/j.jher.2011.07.002

Kinzel, P.J., & Legleiter, C.J. (2019). sUAS-based remote sensing of river discharge using thermal particle image velocimetry and bathymetric lidar. *Remote Sensing*, *11*(19), 2317. https://doi.org/10.3390/rs11192317

Lang, N., Irniger, A., Rozniak, A., Hunziker, R., Wegner, J.D., & Schindler, K. (2021). GRAINet: Mapping grain size distributions in river beds from UAV images with convolutional neural networks. Hydrology and Earth System Sciences Discussions, 25(5), 2567-2597. https://doi.org/10.5194/hess-25-2567-2021

Lee, J. S., & Julien, P. Y. (2006). Electromagnetic wave surface velocimetry*, J. Hydraul. Eng.,* 132(2), 146-153. DOI: 10.1061/(ASCE)0733-9429(2006)132:2(146)

McKenna, S.P., & McGillis, W.R. (2004). The role of free-surface turbulence and surfactants in air–water gas transfer. *International Journal of Heat and Mass Transfer*, *47*(3), 539-553. https://doi.org/10.1016/j.ijheatmasstransfer.2003.06.001

Novak, G., Rak, G., Prešeren, T., & Bajcar, T. (2017). Non-intrusive measurements of

shallow water discharge. *Flow Measurement and Instrumentation* (56), 14–17.

Orlins, J.J., & Gulliver, J.S. (2000). Measurements of free surface turbulence. *Fourth International Symposium on Gas Transfer at Water Surfaces*, June 5-8., Miami Beach, Florida, the USA, 1-7.

Polatel, C. (2006). *Signature of the roughness and the flow regime on the free surface*. Ph.D. thesis, Univ. of Iowa, Iowa City.

Sheng, J., Meng, H., & Fox, R.O. (2000). A large eddy PIV method for turbulence dissipation rate estimation. *Chemical engineering science*, *55*(20), 4423-4434. https://doi.org/10.1016/S0009-2509(00)00039-7

Spada, D., Molinari, P., Bertoldi, W., Vitti, A., & Zolezzi, G. (2018). Multi-temporal image analysis for fluvial morphological characterization with application to Albanian Rivers. *ISPRS International Journal of Geo-Information*, *7*(8), 314. https://doi.org/10.3390/ijgi7080314

Sutarto, T.E. (2015). Application of large scale particle image velocimetry (LSPIV) to identify flow pattern in a channel. *Procedia Engineering* (125), 213 – 219. https://doi.org/10.1016/j.proeng.2015.11.031

Vázquez-Tarrío, D., Borgniet, L., Liébault, F., & Recking, A. (2017). Using UAS optical imagery and SfM photogrammetry to characterize the surface grain size of gravel bars in a braided river (Vénéon River, French Alps). *Geomorphology*, *285*, 94-105. https://doi.org/10.1016/j.geomorph.2017.01.039

Thielicke, W., & Stamhuis, E.J. (2014). PIVlab- Time-Resolved Rigital Particle Image Velocimetry Tool for MATLAB.

Weitbrecht, V., Kühn, G., & Jirka, G.H. (2002). Large scale PIV-measurements at the surface of shallow water flows, *Flow. Meas. Instrum*. (13), 237–245. https://doi.org/10.1016/S0955-5986(02)00059-6

Welber, M., Le Coz, J., Laronne, J.B., Zolezzi, G., Zamler, D., Dramais, G., Hauet, A., & Salvaro, M. (2016). Field assessment of noncontact stream gauging using portable surface velocity radars (SVR).*Water Resour. Res*, (52), 1108–1126. https://doi.org/10.1002/2015WR017906